Title: 1,8-Naphthalimides 3-substituted with imine or β-ketoenamine unit evaluated as compounds for organic electronics and cell imaging

Author: Mateusz Korzec, Sonia Kotowicz, Robert Gawecki, Katarzyna Malarz, Anna Mrozek-Wilczkiewicz [i in.]

Citation style: Korzec Mateusz, Kotowicz Sonia, Gawecki Robert, Malarz Katarzyna, Mrozek-Wilczkiewicz Anna [i in.]. (2021). 1,8-Naphthalimides 3-substituted with imine or β-ketoenamine unit evaluated as compounds for organic electronics and cell imaging. "Dyes and Pigments" (2021), Vol. 0, art. no. 109508, s. 1-22. DOI: 10.1016/j.dyepig.2021.109508

1,8-Naphthalimides 3-substituted with imine or β-ketoenamine unit evaluated as compounds for organic electronics and cell imaging

Mateusz Korzec[a,*], Sonia Kotowicz[a], Robert Gawecki[b], KatarzynaMalarz[b], Anna Mrozek-Wilczkiewicz[b], MariolaSiwy[c], EwaSchab-Balcerzak[a,c], JustynaGrzelak[d], Sebastian Maćkowski[d]

[a]Institute of Chemistry, Faculty of Science and Technology, University of Silesia in Katowice, Szkolna 9, 40-007 Katowice, Poland.
[b] A. Chełkowski Institute of Physics, Faculty of Science and Technology and Silesian Center for Education and Interdisciplinary Research, University of Silesia in Katowice, 75 Pułku Piechoty 1A, 41-500 Chorzów, Poland.
[c]Centre of Polymer and Carbon Materials, Polish Academy of Sciences, 34 M. Curie-Sklodowska Street, 41-819 Zabrze, Poland.
[d] Institute of Physics, Faculty of Physics, Astronomy and Informatics, Nicolaus Copernicus University, 5 Grudziadzka Str., 87-100 Torun, Poland.

Abstract:

In this paper, we describe both new as well as described in our previous works 1,8-naphthalimide derivatives substituted at the 3-C position with imine or β-ketoenamine unitin order to demonstrate a broader scope of research enabling of analysis between the structure-properties relationship relevant to the application of these compounds in organic electronics and cellular imaging. Thermal, physicochemical, optical, electrochemical, electroluminescence, and biological properties of a series of derivatives containing the 1,8-naphthalimideunit were tested and compared. This allowed the determination of impact of substituents in the imide part (hexylamine, phenylethyl, benzyl, fluorobenzyl, methylbenzyl), type of bond (imine or ketoenamine) as well as the substituent on the naphthalene ring (2-hydroxyphenyl, 5-bromo-2-hydroxyphenyl, 3,5-diodo-2-hydroxyphenyl, pyrimidines) on their properties. Moreover, the properties in the aggregating state were tested in the MeOH/PBS system. Imines are susceptible to the hydrolysis process and aggregation-caused photoluminescence quenching(ACQ). In turn, β-ketoenamine shown excited-state intramolecular proton transfer promoted by aggregation (AIEE). Our studies can be helpful in the further design of compounds containing the 1,8-naphthalimide structure for various applications.

1. Introduction

The 1,8-naphthalimide structure is an important building unit for compounds investigated for organic electronics [1-4], ion-selective sensors [5-9], cell imaging [7,10-16], and as the biologically active compounds [10, 17]. The use of this group of compounds in bioimaging is diverse. The naphthalimides with a triple bond attached in the 4-C position tested as well as the naphthalimide Pt(II) complexes tested in bioimaging showed low cytotoxicity and multicolor intracellular fluorescence [18,19]. Imide derivatives were also tested as a spectroscopic probe for studying nucleic acid structure [20]. Moreover, derivatives with the naphthalimide unit were applied in the selective imaging of ions in biological structures, e.g. Zn^{2+} [21-22], Al^{3+} [23] or Cd^{2+} [24]. Their properties in a condensed (aggregative) state and their importance for use in various science areas are also widely discussed [25]. *Aggregation*-induced *emission compounds* (AIEgent) in cellular imaging are also an important subjects studied by many research groups [26-29]. Therefore, the search for AIEgent and its optimization is quite crucial for further development of this area of applications. The properties of compounds can be modulated by changes of linkers or substituents, which is also important in the search for new AIEgens. Therefore, the changes in substituents in the structure favor the preparation of compounds with AIE ability, despite the fact that some of the analogs showed ACQ properties [30-31]. Examples of AIEgent with a 4-substituted 1,8-naphthalimide include: vinyl bond [32], benzaldehyde [33-34] or bromo [35] derivatives, substituted 9,9-bishexylfluorene [36], piperazine [37] or C-O-C [38] linker. Particularly noteworthy are compounds capable of intra molecular proton transfer promoted by aggregation (AIEE) [39-40]. 1,8-Naphthalimides with unsubstituted naphthalene ring have been successfully used in OLEDs [41]. Nevertheless, reports indicate that substituted naphthalimides exhibit better electroluminescent properties [42]. In this regard, tests are carried out on donor-acceptor compounds' properties with a 1,8-naphthalimide system that is key for many applications [43]. In the field of research on the emission mechanisms of 1,8-naphthalimide derivatives, various processes are considered, such as intermolecular charge transfer (ICT) [44], photoinduced electron transfer (PET) inhibition [45-46], excited-state intramolecular proton transfer (ESIPT) process [47], aggregation-induced emission [25] or fluorescence resonance energy transfer (FRET) [48]. The position of substitution 1,8-naphthalimidesis crucial for their properties [49,50]. There are only a few reports on the physicochemical, thermal, electrochemical properties of 1,8-naphthalimidessubstituted at the 3-C

position [1,51-52], while literature concerning 4-substituted derivatives is far richer [8,43,53,54]. Thus, more extensive studies to verify the properties of 3-substituted 1,8-naphthalimidesare required.

In our previous works, we described the susceptibility of the imine bond to hydrolysis [7,52,55-56], while β-ketoenamines are more stable in an aqueous system due to a higher degree of pseudo aromatic nature [52,57]. Therefore, the differences in the properties of these compounds are quite significant for potential use. This paper presents the properties of 3-substituted1,8-naphthalimide derivatives (NIs) with imine or β-ketoenamine bond containing various groups linked with nitrogen in the imide ring. The important properties of these compounds associated with their use in OLEDs as well as cellular imaging were showed. In the paper, thermal, electrochemical and optical properties of1,8-naphthalimideswith imine linkage were compared with their analogues with β-ketoenamine bond [52]. Despite the fact that some of the presented compounds with imine bond have been described in our former work [7], their thermal, electrochemical behavior, and photophysical properties in the solid-state are presented herein for the first time. Additionally, it should be noticed that the electroluminescent properties of both groups (imines and β-ketoenamines derivatives)have not been presented. Moreover, biological tests for the β-ketoenamine series were performed compared with reported results for imine derivatives [7].

2. Discussion of results

2.1.Characteristics of 1,8-naphthalimide derivatives

The 1,8-naphthalimides were obtained in a three-step synthesis, starting from 3-nitronaphthalic anhydride according to the method described in our previous publications [1,7,52]. The chemical structure of the discussed compounds is presented in Fig. 1. The compounds denoted as **a**, **b**, **c** or **d** contain an azomethine or β-ketoeamine bond, respectively. The synthesis and structural characterization of compounds **1a**, **1b**, **1c**, **3a** and **1d**, **2d**, **3d**, **4d**, **5d** were presented in our previous works [7,52], while ^{1}H, ^{13}C NMR spectra and an elemental analysis for other molecules (**2a**, **2b**, **2c**) are given in the Supplementary Information.

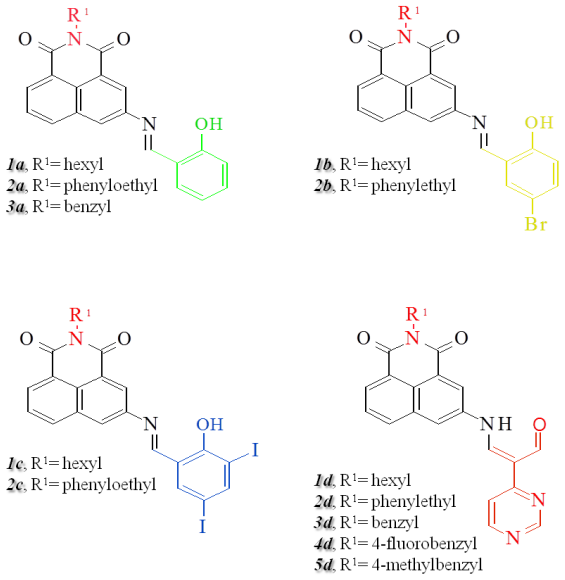

Figure 1. Structures of the compounds.

The tested compounds are analogues to each other, mainly due to the keto-enoltautomerism occurring in the imines [7]. The presence of electron withdrawing -Br and -I substituents affect the stabilization of the ketoenamine form, therefore these compounds partially exhibit properties typical for this group.

2.2.Thermal properties

The 1,8-naphthalimide derivativeswere subjected to thermogravimetric (TGA) and differential scanning calorimetry (DSC) analysis. Thermal stability tests were performed for all imines, and the results are summarized in Table 1, while the thermal properties of β-ketoenamines were presented in our previous publication [52]. The DSC thermograms of imines are presented in Fig. S2 in the Supplementary Information.

Table 1. Thermal properties of 1,8-naphthalimide derivatives.

Code	*TGA*			*DSC*			
				I heating scan	II heating scan		
	T_5 [°C]	T_{10} [°C]	T_{maks} [°C]	T_m[°C]	T_g[°C]	T_c [°C]	T_m [°C]
1a	312	328	375	128	19	nd	nd
1b	322	332	357	153	36	124	153
1c	300	319	357	196	75	nd	nd
2a	332	349	391	194	57	125	193
2b	321	331	345	202	72	180	203
2c	310	321	325	257	108	198	255
3a	325	339	400	219	72	nd	nd

T_5, T_{10} - temp. of 5% and 10% weight loss from TGA curves, $T_{max.}$- temp. of the maximum decomposition

rate from DTG curves, $\mathbf{T_m}$- Melting temp., $\mathbf{T_g}$ - Glass transition temp., $\mathbf{T_c}$ – Cold crystallization temp.,***nd***-not detected.

The imines showed high thermal stability, and 5% weight loss occurred above 300°C and was characterized by one-stage thermal decomposition (see Fig. S1). The obtained compounds have a crystalline character and the presence of the aryl substituent in the imide part favorably increased the T_m. In the second heating scan of all molecules exhibited the glass transition temperature (T_g) and they can form glassy phases above room temperature, except for **1a**. The compounds containing aliphatic substituents within the imide, i.e., **1a** and **1b**, showed lower T_g compared to others. It can be noticed that the presence of iodine atoms (**1b** and **2b**) increased the T_g compared to Br atom (**1c** and **2c**). The imines **1a**, **2c**, and **3a** form stable amorphous molecular materials because further heating above their T_g yields no peaks due to crystallization and melting,unlike for the others, which crystallized and then melted again (see Table 1, Fig. S2). Analyzing the results for **1a**, **1b**, **1c**, as well as **2a**, **2b**, **2c**, it can be seen that the electron-acceptor substituent (-Br, -I) in the 2-hydroxyphenyl ring affects the thermal properties of the compound (see Table 1). Therefore, the presence of -I and -Br atoms compared to the unsubstituted 2-hydroxyphenyl ring causes an increase in the temperatures of these phase transitions. The influence of the electron-acceptor substituent on the thermal properties may be associated with the formation of the keto-enamine form, the presence of which would explain the observed regularities. This is beneficial when designing chemical structures of compounds for potential use in organic electronics.

2.3.Electrochemical properties

The electrochemical behavior of presented compounds was examined cyclic voltammetry (CV). Specifically, two crucial parameters for materials considered for organic electronics were examined, i.e., ionization potential (IP) and electron affinity (EA) related to HOMO and LUMO levels, respectively. IP and EA were calculated from the first redox couple corresponding to the first oxidation and the first reduction (means onset potentials) of the neutral molecule to a radical cation and anion. The electrochemical properties of imines are given in Table S2, and showed in Fig. S3, while the results obtained for β-ketoenamines were described in our previous work [52].

The first reduction peak (E_{red}) can be found in the range -1.76 –-1.51 V (see Table S2), which can suggest that the negative charge is localized on the –CH=N– unit in the first step, as

was reported in [58] for other NIs derivatives. Furthermore, the 1,8-naphthalimide half-peak potential of the reduction process was reported in the literature to be −1.71 V vs. Fc/Fc^+ [1]. The irreversible process was seen for the first reduction and quasi-reversible for the second reduction. The electron-donating units raise the HOMO energy, while electron-withdrawing groups reduce the LUMO energy, influencing the value of the band gap. Ionization potential and electron affinity values (see Table S2) are affected by the *N*-substituent and by structures coupling *via* imine linkage. However, for the investigated type of compounds, a more profound effect was observed on the EA value as it changes within the range of 0.31 V, while the IP value changes within the range of 0.12 V. Similar effect was seen for derivatives described in [1]. The alkyl or phenyl group would lead to a more electron-rich aromatic system than unsubstituted compound (electron-donating effect), and halogen substituents have a high electronegativity and bonded to the aromatic ring exert an inductive electron withdrawal. The electrochemical band gaps are similar in the group of compounds with the same substitutes coupling *via* imine linkage and E_g value decreasing in order OH < Br < I. Comparing **1c** and **1a**, the lack of iodine substituents increased the EA value and decrease of the IP, and the observed E_g raised markedly (from 2.32 to 2.51 eV). Halogen substituents in compounds **1c**, **2c**, **1b**, and **2b** shift the reduction potential to less negative values than compounds **1a** and **2a**, in agreement with the expected improved delocalization of the negative charge over the molecules.

2.4.Optical properties

The optical properties of most imines and all β-ketoenamines in various solvents were shown in our previous publications [7,52]. Therefore, in this part, we present the results covering the properties of compounds dissolved in chloroform and in the solid-state as a thin film on the glass substrate. Additionally, the photoluminescence (PL) of compounds molecularly dispersed (2 wt.%) in a matrix (poly(9-vinylcarbazole) (PVK) (50 wt.%) :2-(4-biphenylyl)-5-(4-tert-butylphenyl)-1,3,4-oxadiazole(PBD)(50 wt.%)) was examined because the layers of the same composition were used for testing of electroluminescence (EL) ability of investigated compounds. The compounds in a binary MeOH/PBS mixture (0.1 M) with different PBS content were also tested.

The obtained spectroscopic data in the chloroform solution and in the solid-state are listed in Table 2, whereas in Fig. S4 and S5, the UV–Vis and PL spectra are presented.

Analyzing Fig. S4 and the values in Table 2 we noticed that the substituent mainly influences the electronic absorption properties in the part of the naphthalic ring. The influence of the substituent in the imide part plays a much smaller role. In the case of 1,8-naphthalimides with imine linkage, N-substituted with 2-hydroxyphenylunit (series **a**) three maxima are visible at ca. 287, 315, and 340 nm, with the main band at 340 nmdue to n-π^* transitions in the imide unit [1,7].The substitution of the imide nitrogen with 5-bromo-2-hydroxyphenyl (series **b**) also gives an absorption band with three maxima, with the most intense localizedat 310 or 316 nm. However, in the case of series **c** with 3,5-dijodo-2-hydroxyphenylone maximum at 317 nmwas seen.Such visible changes are associated with ketone-enol tautomerism, where the presence of electron-withdrawing atoms promotes the formation of the ketoenamine form (-Br or -I) [7]. The absorption spectra in the film exhibited the red shift of λ_{max} compared to the chloroform solution (see Table 2, Fig. S4b). In the case of PVK:PBD:compounds blends characteristic shoulders of PVK and PBD in the UV-Vis spectra are seen [1].

In the chloroform solution, the imines emitted light with maximum PL band (λ_{em}) in the green spectral region (520–528 nm), while λ_{em} of β-ketoenaminesislocatedin the blue spectral region (470–474 nm) (see Table 2, Fig. S5a). In the film, theλ_{em} are bathochromically shifted with respect to the solution and are in the range of 536–582 nm for imines and 527–545 nm for β-ketoenamines. The calculated Stokes shift for the β-ketoenamines (7632–7721 cm^{-1}) was smaller than for the azomethines (10181–12507 cm^{-1}), which may indicate that the changes of the dipole moments in the ground (S_o) and excited (S_1) state are smaller forβ-ketoenamines.

Table 2. UV–Vis and PL spectroscopic parameters of the investigated compounds.

Code	*Medium*	*UV-Vis*	*PL*						
		λ_{max} *[nm]*	λ_{em} *[nm]*	*StokesShift[c] [cm^{-1}]*	Φ *[%]*	τ_{eff} *[ns]*	X^2	$k_r \cdot 10^{6d}$ *[s^{-1}]*	$k_{nr} \cdot 10^{6d}$ *[s^{-1}]*
1a	$CHCl_3$[7] [a]	287, 316, 340, 373^{sh}	520	10181	13.09	20.78	1.047	6.30	41.8
	Film	350, 397^{sh}	464^{sh},**540**, 576^{sh}	10053	2.86	3.32	0.998	8.61	292.6
	Blend PVK:PBD[b]	310^{sh}	**378**, 390^{sh}, 495^{sh}	-	5.99	-	-		
		350^{sh}		-	6.92	-	-		
2a	$CHCl_3$ [a]	290, 315, 340, 373^{sh}	520	10181	2.37	20.42	0.944	1.81	47.2
	Film	320, 348, 392^{sh}	464^{sh}, **538**, 570^{sh}	12663	1.40	2.56	0.891	5.47	385.2
	Blend PVK:PBD[b]	310^{sh}	**378**, 390^{sh}, 491^{sh}	-	1.94	-	-		
		350^{sh}		-	3.85	-	-		
3a	$CHCl_3$[7] [a]	285, 314, 340, 372^{sh}	526	12354	5.74	20.34	0.898	2.82	46.3
	Film	320, 346, 386^{sh}	463^{sh}, **536**, 570^{sh}	12593	1.55	29.78	0.932	0.52	33.1
	Blend PVK:PBD[b]	310^{sh}	**378**, 392^{sh}, 478	-	10.46	-	-		
		350^{sh}		-	16.25	-	-		
1b	$CHCl_3$[a]	310, 340, 375^{sh}	523	10291	5.25	20.79	1.083	2.53	45.6
	Film	324, 380^{sh}	464^{sh}, **555**, 585^{sh}	12846	2.48	3.48	0.939	7.13	280.2
	Blend PVK:PBD[b]	310^{sh}	**379**, 390^{sh},488^{sh}	-	4.47	-	-		
		350^{sh}		-	6.15	-	-		
2b	$CHCl_3$[a]	316, 340, 373^{sh}	520	10291	2.00	20.21	1.022	0.99	48.5
	Film	318, 383^{sh}	464^{sh}, **550**	13265	1.45	2.00	0.858	7.25	492.8
	Blend PVK:PBD[b]	310^{sh}	**379**, 392^{sh}, 489^{sh}	-	2.29	-	-		

		350[sh]		-	5.54	-	-		
1c	$CHCl_3$[a]	317, 370[sh]	528	12507	3.09	20.91	1.002	1.48	46.3
	Film	325, 386[sh]	464[sh], ***580***	13528	0.82	0.17	0.975	48.24	5834.1
	Blend PVK:PBD[b]	310[sh]	**379**, 392[sh], 398[sh]	-	3.6	-	-		
		350[sh]		-	3.3	-	-		
2c	$CHCl_3$[a]	318, 372[sh]	520	10913	1.02	21.55	0.989	0.47	45.9
	Film	325, 390[sh]	415, 450[sh],**582**	13587	0.21	4.00	0.968	0.53	249.5
	Blend PVK:PBD[b]	310[sh]	**383**, 497[sh]	-	2.88	-	-		
		350[sh]		-	4.08	-	-		
1d	$CHCl_3$[35] [a]	285, 345, 407[sh]	470	7709	5.59	2.43	0.947	23.00	388.5
	Film[35]	302,348, 420[sh]	527	9596	3.27	12.49	0.989	2.62	77.4
	Blend PVK:PBD[b]	310[sh]	**380**, 488[sh]	-	4.13	-	-		
		350[sh]		-	4.65	-	-		
2d	$CHCl_3$[35] [a]	287, 347, 407[sh]	472	7632	7.69	4.3	0.994	17.88	214.7
	Film[35]	350, 420[sh]	530	9704	3.54	11.29	0.867	3.14	85.4
	Blend PVK:PBD[b]	310[sh]	**392**, 455[sh], 500[sh]	-	1.96	-	-		
		350[sh]		-	5.62	-	-		
3d	$CHCl_3$[35] [a]	285, 348, 407[sh]	473	7676	6.69	2.89	1.034	23.15	322.9
	Film[35]	345, 420[sh]	545	10637	3.22	8.44	0.961	3.82	114.7
	Blend PVK:PBD[b]	310[sh]	**395**, 453[sh], 503[sh]	-	4.03	-	-		
		350[sh]		-	5.15	-	-		
4d	$CHCl_3$[35] [a]	287, 347, 407[sh]	474	7721	10.79	4.6	0.960	23.46	193.9
	Film[35]	347, 420[sh]	524	9735	2.24	6.98	0.917	3.21	140.1
	Blend PVK:PBD[b]	310[sh]	**386**, 497[sh]	-	7.35	-	-		
		350[sh]		-	7.41	-	-		
5d	$CHCl_3$[35] [a]	290, 348, 409[sh]	470	7542	8.15	2.55	0.956	31.96	360.2
	Film[35]	340, 354[sh],435[sh]	532	10650	3.30	7.34	0.945	4.50	131.7
	Blend PVK:PBD[b]	310[sh]	**386**,496[sh]	-	3.58	-	-		
		350[sh]		-	4.72	-	-		

[a] $c=10^{-5}$[mol/dm^3], [b] 2wt% concentration of the compound in PVK:PBD (50wt%:50wt%), [c] Stokes shifts calculated according to the equation $\Delta\nu=(1/\lambda_{abs}-1/\lambda_{em})\cdot10^7$ [cm^{-1}], [d] k_r as the radiative and k_{nr} as the non-radiative decay rates calculated according to the equations: $k_r = \Phi/\tau_{eff}$; $k_{nr} =(1-\Phi)/\tau_{eff}$, [sh] – shoulder, Underlined data indicates the dominant band. Bold data indicates the most intense PL.

The impact of the electron-withdrawing groups on the maximum emission bands in the solid-state was visible. Unsubstituted 2-hydroxyphenol emitted light with the maximum in the range of 536– 540 nm, substitution with bromine caused a slight shift to 550– 555 nm, while the presence of iodine shifts the λ_{em} to 580– 582nm (see Table 2 and Fig. S5b). On the other hand, in the PL spectrum of the compounds (2wt%) blended with PVK:PBD the λ_{em} (at 379– 395 nm) typical for the matrix are dominated and weak structured band at about 490 nm is seen. Only in the case of molecule **3a** an additional band with a maximum at 478 nm, indicating a partial charge transfer from the host to the guest (see Fig. S5c) is observed.

The fluorescence lifetime (τ_{eff}) in the chloroform solution is longer for the imine derivatives (approx. 20 ns) compared to the β-ketoenamines(2.43 – 4.6 ns), the same tendency was reported in the publication [52]. Moreover, the obtained lifetimes (in ns)were recorded as the mono-exponential curves indicate the emission from the first singlet excited state ($k_r= 10^6$ s^{-1}) [52]. An inverse relationship was observed for the thin films, where longer lifetimes were recorded for β-ketoenamines (6.98 – 12.49 ns). The exception is compound **3a**, which in the solution and in the solid-state exhibited similar PL lifetimes values were obtained. The fluorescence quantum yields (Φ_{PL}) in the solutions are typically lower for imines (1.02 –

13.09%, and for β-ketoenamines 5.59 – 10.79%) and the same trend was observed for the thin films (comparing imines and β-ketoenamines with the chloroform solution). Furthermore, in the case of imines, the presence of the electron-withdrawing group, especially iodine, significantly reduces the PL quantum yields of the compounds. It may also be due to the spin-orbit coupling (the internal heavy atom). It can be seen for the both groups of the molecules with the hexyl substituent: **1a** (2.86%), **1b** (2.48%), **1c** (0.82%) as well as with the phenylethynylunit: **2a** (1.40%), **2b** (1.45%), **2c** (0.21%). The radiative (k_r) and non-radiative (k_{nr})decay rates were calculated based on the lifetime and quantum yields. The non-radiative processes dominate for all tested compounds ($k_{nr}>k_r$), which indicates that the deactivation of the excited states is largely carried out e.g. by internal conversion (IC) [52]. β-Ketoenamines exhibited more radiation processes in the case of solutions than in the form of thin layers, opposite behavior is noticed for azomethines (except **3a**).A significant low k_{nr} value was obtained for **1c** (k_{nr}=5834.1 s^{-1}) in the form of the thin film, which means that the deactivation of the excited states, in this case, takes place primarily in non-emissive pathways.

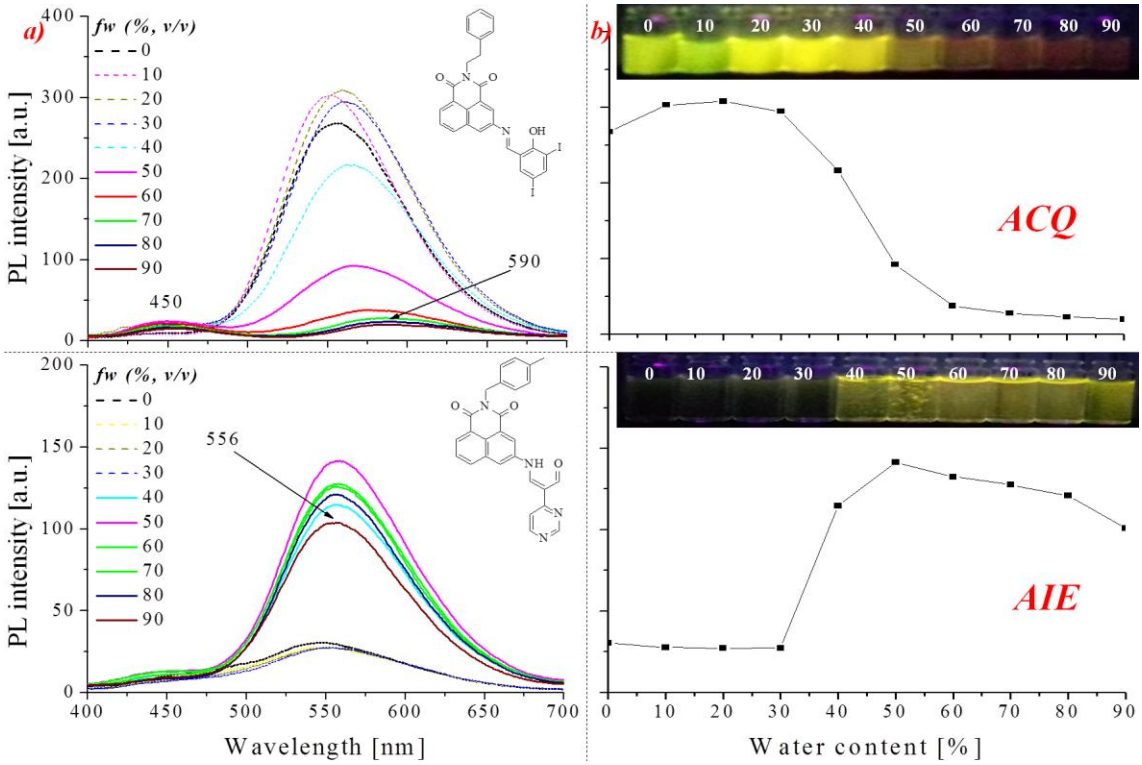

Figure 2. Photoluminescence (PL) properties of imine**2c** and β-ketoenamine**5d** by concentration 25 μM: *(a)* in a binary mixture of MeOH/PBS (fw: 0.1 M PBS, v/v) with an increasing water (PBS) content (*fw*), (*b*)λ_{em} intensity versus the water content (*fw*) in the solvents mixture. Photographs were taken under 366 nm UV irradiation from a hand-held UV lamp.

Further studies of 1,8-naphthalimide derivatives photoluminescence properties under λ_{ex} = 366 nm were performed in the MeOH/PBS(0.1 M) mixture with various PBS content in the system. The concentration of the compounds in MeOH/PBS was 25 μM, which corresponds to the concentration used for live cell imaging investigations. In the first stage, the changes in emission of solutions under a UV lamp (λ_{ex} = 366 nm) occurring after every 10 minutes up to 80 minutes were documented by photographs. Next, the PL spectra of 2 hours after preparation of solution the photoluminescence spectra were performed using excitation wavelength of 360 nm. The observed temporal changes in PL spectra of azomethines (see Fig. S6), may be due to partial hydrolysis [52] and/or to the excited-state intramolecular proton transfer (ESIPT) assisted solvent [7]. In the systems with less than 50% content of water (see Fig. 2 and Fig. S9), the quenching of emission associated with compound aggregation (ACQ) is noticeable. In the case of β-ketoenamines, changes over time are negligible (see Fig. S7). In the systems with higher water content, at the beginning an increase in the emission due to aggregation (AIE) can be seen (see Fig. 2 and Fig. S9). Moreover, the presence of the second band is visible at approx. 450 nm (see Fig. 2 and Fig. S7), which is related to the ESIPT process promoted by aggregation phenomena (AIEE) [59-60].

2.5. Electroluminescene

Electroluminescence (EL) ability of 1,8-naphthalimide derivatives was examined in the devices with the following configuration ITO/PEDOT:PSS/PVK:PBD:compound(2 or 15 wt.%)/Al (see Fig. 3a). The active layer of the devices consists of 1,8-naphthalimide dispersed molecular in a binary matrix PVK:PBD with an equal weight ratio (50:50wt.%). The diodes with neat compounds as the active layer were also prepared (ITO/PEDOT:PSS/compound/Al).

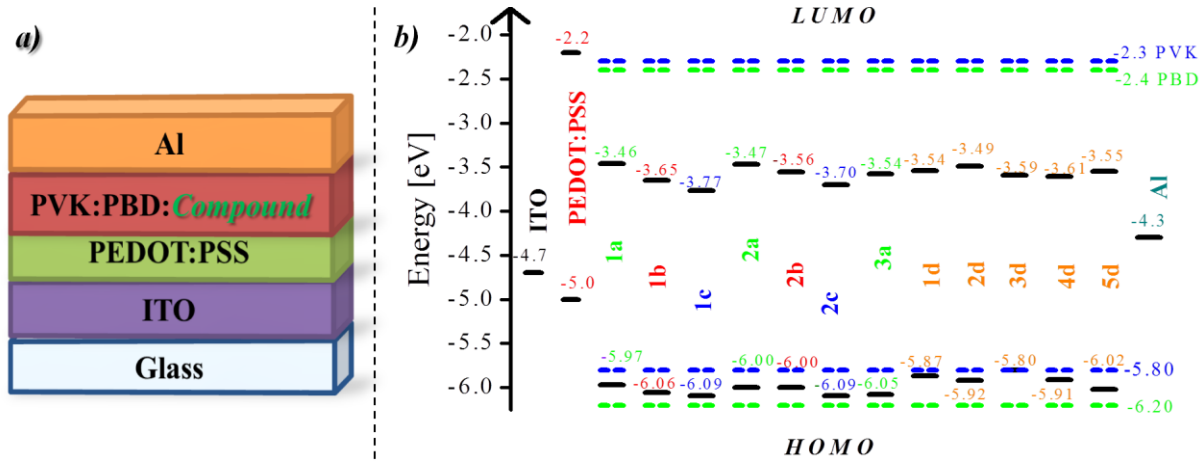

Figure 3.*(a)*Device structure and *(b)*HOMO and LUMO energy levelsofdiode components with respect to the vacuum level.

However, in such a configuration only two devices with **3a** and **1c** showed EL with maximum emission band (λ_{EL}) at 663 and 711nm, respectively (see Fig. 4). The electroluminescence spectra of the rest of the diodes are presented in Fig. 4as well as in the Supplementary Information in Fig. S10. The fabricated diodes with PVK:PBD matrices possess the guest-host structureand the energy transfer from host (PVK:PBD) to guest (1,8-naphthalimide derivatives)via Förster or Dexter mechanism can occur [61]. In such devices the charge trapping mechanism, the formation of excitons directly in luminophore, can also occur [62-63]. Both series of 1,8-naphthalimides, that isimines and β-ketoenamines, exhibit LUMO and HOMO levels, which are not suitably matched to frontier molecular orbitals energy levels of PVK and PBD (see Fig. 3b),which means, that the Dexter mechanisms is unlikely to occur. In such a case, the charge trapping mechanism should be dominant [64-65]. Considering the UV-Vis spectra of 1,8-naphthalimide derivatives and PL spectrum of a matrix (see Fig. S4 and S5), it can be expected that the energy transfer from host to guest (1,8-naphthalimide derivatives)via Förster process is possible but should be inefficient due to only partial overlapping of these spectra. The efficient energy transfer from the host to the guest via Förster mechanism is possible if the PL spectrum of the host overlaps with electronic absorption spectrum of the guest [65].

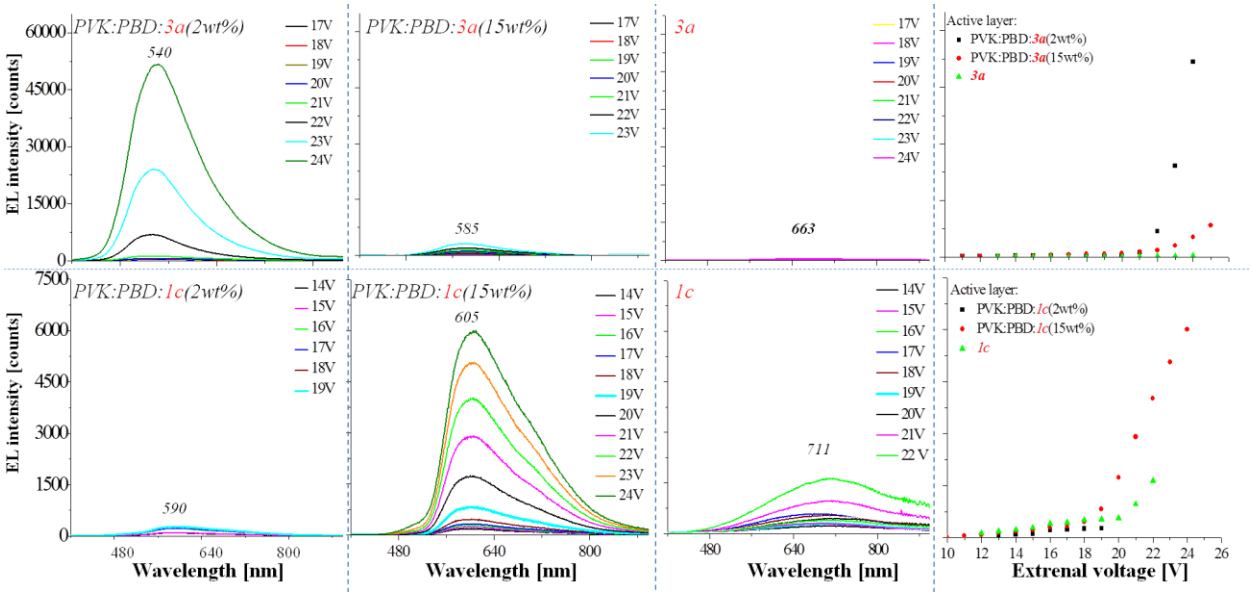

Figure 4. Electroluminescence (EL) spectra of **3a** and **1c**withEL-voltage curve.

In the PL spectra of 1,8-naphthalimide derivatives blended with PVK:PBD the emission of the matrix was dominant (see Fig. S4 and S5). Only in the case of PL spectrum of **3a** (2 and 15wt.%) in PVK:PBD, the λ_{em} assigned to emission of 1,8-naphthalimide was seen, which confirms that inefficient Förster mechanism can occur [61,65]. All fabricated devices with the guest-host structure emitted light under external voltage from green to orange spectral region with various intensity (see Fig. 4, S10 and S11). The increase of naphthalimide content in PVK:PBD matrix (from 2 to 15wt.%) affected on the position of λ_{EL} and also its intensity. Devices with the 15wt.% content of **2b**, **1c**, **3d**and **4d** in the active layer exhibited the strongest intensity of EL compared with the diodes with 2wt.% (see Fig.S10 and S11). Additionally, the bathochromic shift of λ_{EL} for 15 wt.% of all compounds compared with the devices with 2 wt.% is seen. Taking into account the diodes with **3a** and **1c** depending on the device structure and compound content in a matrix, the color of emitted light changed from green through yellow to red for **3a** and from yellow through orange to red spectral region for **1c** (see Fig. 4). The highest intensity of EL was registered for the diode with active layer PVK:PBD: imine **3a** 2wt.%, for 24V (EL intensity – 50568 counts, see Fig. 4). It should be noticed, that only basic research concerns EL ability, based on registration of EL spectra are showed herein. Based on presented preliminary results, the most perspective for further investigations seem to be 1,8-naphthalimide **3a**, **1c** and **2d**.

2.6. Biological studies

Taking into account the interesting optical properties of the obtained 1,8-naphthalimide derivatives, we decided to assess their behavior in the biological system and the possibility of using them as cellular dyes. For typical promising fluorescent dyes, it is important to combine several valuable parameters such as large Stokes shift (over 80 nm), absorption over 340 nm increasing the signal-to-noise ratio, strong fluorescence, high quantum yield and low photobleaching. In addition, pharmacokinetic properties such as appropriate lipophilicity, metabolism, interaction with proteins or ions chelation allow for a specific staining effect and high quality of images, which is extremely important in bioimaging applications [66]. On the other hand, fluorescent dyes with high photostability and relative low toxicity are beneficial to long term staining in cellular system [67]. For this reason, first of all, we determined the antiproliferative activity of tested compounds using a colorimetric MTS assay based on tetrazolium salt. The tests were carried out on cell lines derived from the two the most common cancers in the whole population: the colorectal cancer - HCT 116 cell line and the breast cancer - MCF-7 cell line. The results as IC_{50} values, defined as the concentration of compound required for 50% inhibition of cell proliferation, are presented in Table 3.

Table 3. Antiproliferative activity of tested compounds against colon (HCT 116) and breast (MCF-7) cell lines.

code	*LogP*[a]	*Activity - IC_{50} [µM]*	
		HCT 116	*MCF-7*
1a*	4.72 ± 0.93	>25	>25
1b*	5.92 ± 0.97	>25	>25
1c*	7.26 ± 1.02	>25	>25
1d	2.26±0.94	>25	>25
2	2.10 ± 0.85	>25	>25
2a	4.25 ± 0.93	>25	>25
2b	5.46 ± 0.98	19.86 ± 1.55	16.16 ± 0.65
2c	6.79 ± 1.02	>25	>25
2d	1.79± 0.94	>25	>25
3a*	3.84 ± 0.94	24.76 ± 2.86	>25
3d	1.38±0.94	>25	>25
4d	1.43± 0.98	>25	>25
5d	1.84±0.94	>25	>25

*data from [7]

[a]*LogP* - partition coefficient between octanol and water, calculated in ACD/ChemSketch

In general, all tested 1,8-naphthalimide derivatives after 72h incubation at 25 μM concentration did not show any cytotoxicity against cancer cells. The exception was azomethine **2b**, which had a slight effect on HCT 116 and MCF-7 cells viability (calculated IC_{50} was 19.89 μM and 16.16 μM, respectively). However, due to the time of staining and the fact that tested compounds reach the maximum fluorescence level (1-2h) relatively quickly, these concentrations are acceptable for further bioimaging experiments.

In the next step we conducted a series of imaging experiments on MCF-7 cells, which determined the use of synthesized azomethines and β-ketoenamines as fluorescent dyes. As it was shown in spectrophotometric studies, the absorption profile of the tested compounds allow only on excitation with DAPI filter (excitation at 330-380 nm wavelength). The images of alone azomethines (**2a**, **2b**, **2c**) and β-ketoenamines (**2d**, **4d**, **3d**, **5d**) are presented in Fig. 5 and Fig. 6 (first panel). In general, we observed the different behavior of two groups of analyzed 1,8-naphthalimide derivatives in the cellular context, which was also confirmed by earlier studies of aggregation properties in this and our previous works [7,52]. In case of azomethines based on phenylethylamine moiety, it seems that the ability to hydrolysis was decisive for strong fluorescence in cells. This fact is confirmed by staining cells with **2a-c** derivatives and the corresponding substrate - phenylethylamine (**2**). As presented in Fig. 5, the strong green fluorescence were recorded only for **2** and **2c** compounds. Therefore, we assume that only the iodine-derivative (**2c**) can hydrolyze to amine in biological systems. In turn, the high ability to aggregate in a cellular environment can suppress the fluorescence of rest of compounds containing 2-hydroxyphenyl (**2a**) and 5-bromophenyl (**2b**) groups (low fluorescence signal were registered). These observations are surprisingly to our previous results for azomethines based on hexylamine, where we indicated that derivatives with phenyl (**1a**, **1b**) substituents have a strong fluorescence and probably higher hydrolysis capacity than 3,5-diiodine (**1c**) [7]. Moreover, the weak fluorescence signal and low quality of the micrograph was observed for derivative based on benzylamine moieties with 2-hydroxyphenyl group (**3a**) [7].These results for azomethines may suggest, that replacement of aliphatic hexylamine by aryls moieties such as phenylethyl- or benzylamine for compounds containing phenyl group, may have a negative effect and cause strong fluorescence quenching in cells.

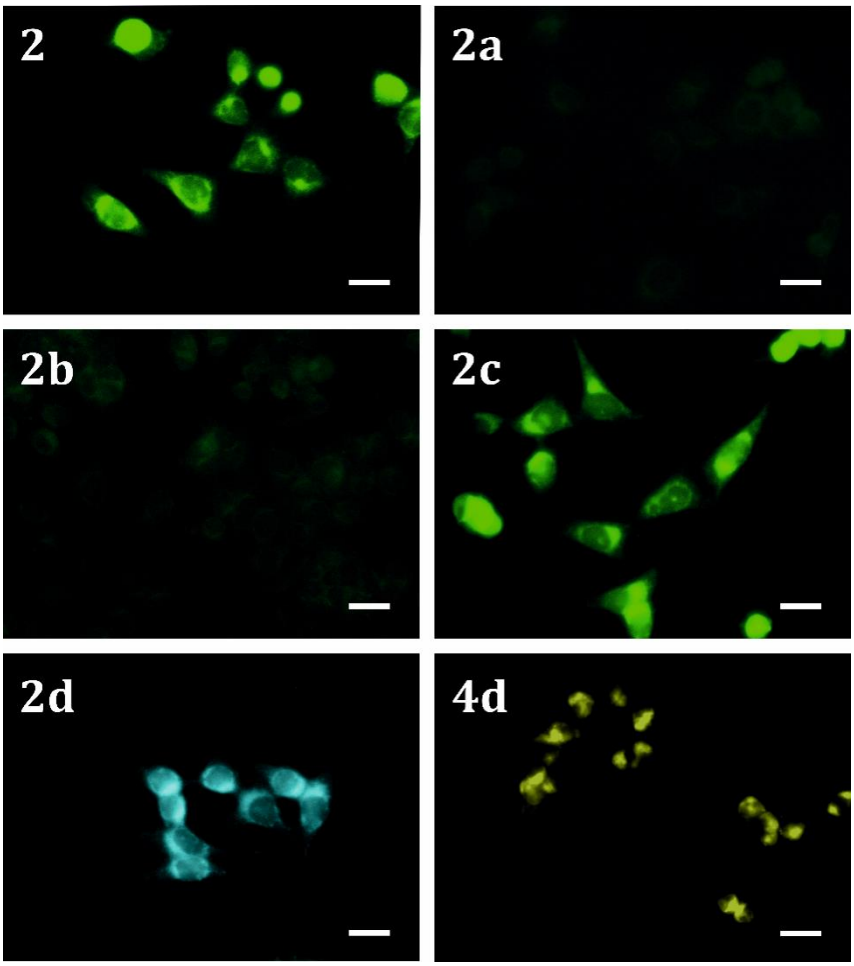

Figure 5. Fluorescence images of MCF-7 cells stained with **2**, **2a-d**, **4d**compounds. Scale bars indicate 50 μm.

The opposite situation was observed in the case of β-ketoenamines, which promote fluorescence in the biological environment through strong aggregation process. Most of them are characterized by a large Stokes shift, which allows to observe very high blue/green or yellow fluorescence in cells. The spectroscopic data and aggregation tests partially confirm these results, but in case of one compounds (**1d**) we observed different behavior during bioimaging experiments. On the basis of the measured optical parameters, it seems that β-ketoenamine **1d** containing the hexylamine chain in the imide part has a greater ability to aggregate and thus fluorescence in a system reflecting the cellular conditions, in which the water content is over 60% (see Fig. S8). However, bioimaging studies revealed that **1d** does not exhibit any fluorescence in cells (data not shown). This phenomenon may be explained by the fact that the compound probably does not pass through the cell membrane or is quickly excreted by drug efflux transporters. At this point it is worth emphasize that changes of substituents in the benzyl

ring in the imide part of β-ketoenamines do not influence their fluorescence intensity, but may significantly affect the selectivity of their accumulation in cells. Preliminary observations apparently indicated that two tested derivatives tend to accumulation in membranous structures in cells. In order to confirm these assumptions, we have performed co-localization experiments of the tested compounds with commercial dyes specific for mitochondria (MitoTracker Orange/Green), lysosomes (LysoTracker Red) and endoplasmic reticulum (ER-Tracker Red). In case of **2d** and **4d** derivatives, it can be concluded that they are more evenly distributed between those organelles and do not exhibit selective accumulation. In contrast, benzyl- (**3d**) and methylbenzylamine (**5d**) derivatives have a clearly increased affinity to the negatively charged mitochondrial membrane, as presented in Fig. 6. Interestingly, these derivatives also localized more selective than azomethines based on hexylamine chain, which partially accumulated in mitochondria and endoplasmic reticulum [7].

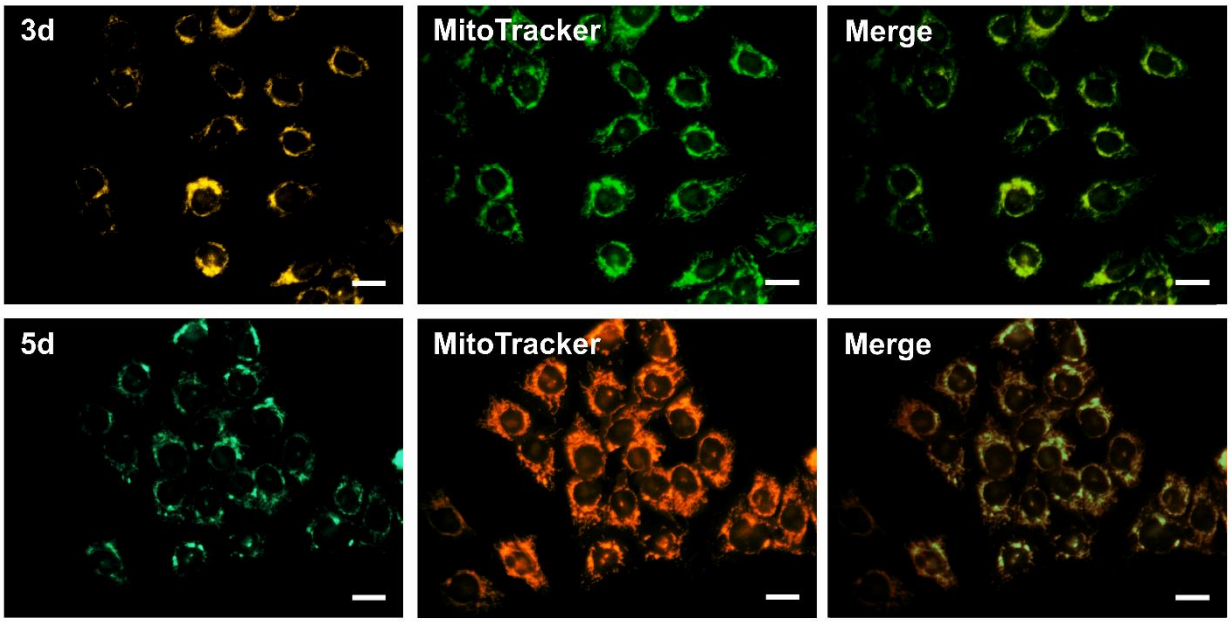

Figure 6. Colocalization images of **3d**, **5d** compounds (first panel) and MitoTracker Green/Orange dye (middle panel) in MCF-7 cells. Scale bars indicate 50 μm.

3. Conclusions

The properties of 1,8-naphthalimide derivatives containing at 3-position an imine (7 compounds) or β-ketoenamine (5 compounds) bond and substituted by various unit in both imide ring and naphthalene part were tested and compared. The scope of the research included study of

thermal, electrochemical, UV-vis, emission, electroluminescence and biological properties. The effect of structural factors on the crucial properties for applications in organic electronics and live cell imaging was shown was analyzed. All investigated 1,8-naphthalimide (imine and β-ketoenamine) appear as a crystalline form and can be easily transformed into molecular glasses (II heating scan in DSC).It was noted that the thermal stability was increased with the aryl substituents (benzyl or fenyloetyl) in the imide part as well as with the presence of the β-ketoenamine bond in the structure. This applies to both the β-ketoenamines themselves as well as the iodine-substituted imines (**1c** and **2c**) where enole-ketone tautomerism occurs. The electrochemical measurement demonstrates that n- and p-type doping to the conducting state of these compounds is achievable. Moreover, all compounds showed the E_g value below 3 eV, that required for organic electronics. Halogen substituents in imines significantly shifted the reduction potential to less negative value and decreased the electrochemical band gap. The light-emitting ability of the investigated molecules in solution and in condensed phase was demonstrated. For the imines containing the substituent I- (**1c**, **2c**), the fluorescent quantum yield in the film was significantly lowered. The EL studies showed that all β-ketoenamines showed electroluminescence properties at low current voltages (ca. 10 V). On the other hand, in the case of the tested imines, one (**3a**) showed excellent electroluminescent properties. All compounds tested are biologically inactive but they show ability to live cells imaging. Compounds with imine are prone to hydrolysis to form an amine capable of imaging cellular structures on green color. However, the β-ketoenamines show greater stability in the water and undergo aggregation process responsible for live cell imaging on blue/green/orange-yellow color. The extension of research on naphthalimide derivatives substituted in the 3-position is necessary to understand the nature of these compounds, despite the extensive knowledge about the derivatives in the 4-position. Apart from the push-pull effects, other properties, such as the ability to AIE, may determine the applicability of the compounds. Therefore, the investigations of such molecules is an important direction in the search for new useful derivatives with a 1,8-naphthalimide unit.

Acknowledgments

The research was partially financed by the National Science Centre (Poland) within the OPUS grant 2017/27/B/ST3/02457 (SM, JG). The biological studies was supported by the National Science Centre grant 2019/35/B/NZ5/04208 (KM).

References

1. S. Kotowicz, M. Korzec, M. Siwy, S. Golbac, J.G. Malecki, H. Janeczek, S. Mackowski, K. Bednarczyk, M. Libera, E. Schab-Balcerzaka, *Dyes and Pigments.* 2018, **158**, 65.
2. J.A. Gan, Q.L.Song, X.Y. Hou, K. Chen, H.Tian, *Journal of Photochemistry and Photobiology A: Chemistry. 2004*, **162**, 399.
3. T.T. Do, S. Chavhan, J. Subbiah, T.H. Ou, S. Manzhos, D. Jones, J.M. Bell, J.H. Jou, P. Sonar, *New J. Chem.*, 2019, **43**, 9243.
4. M. Zhu, J. Miao, Z. Hu, Y. Chen, M. Liu, I. Murtaza, H. Meng,*Dyes and Pigments.* 142, 2017,**142**, 39.
5. S.Fernández-Alonso, T.Corrales, J.L.Pablos, F.Catalina,*Sensors and Actuators B: Chemical*, 2018,**270**, 256.
6. Y.K. La, J.A. Hong, Y.J. Jeonga, J. Lee, *RSC Adv.*, 2016, **6**, 84098.
7. M. Korzec, K. Malarz, A. Mrozek-Wilczkiewicz, R. Rzycka-Korzec, E. Schab-Balcerzak, J. Polański,*Spectrochimica Acta Part A: Molecular and Biomolecular Spectroscopy*, 2020, **238**,118442.
8. D. Liu, H. Zhu, J. Shi, X. Deng, T. Zhang, Y. Zhao, P. Qi, G. Yang, H. He., *Anal. Methods*, 2019, **11**, 3150.
9. T.S. Reddy, R. Maragani, R. Misra, *Dalton Trans*., 2016, **45**, 2549.
10. S. Banerjee, E.B. Veale, C.M. Phelan, S.A. Murphy, G.M. Tocci, L.J. Gillespie, D.O. Frimannsson, J.M. Kelly, T. Gunnlaugsson, *Chemical Society Reviews*, 2013,**42**, 1601.
11. X. Liu, F. Gu, X. Zhou, W. Zhou, S. Zhang, L. Cui, T. Guo, *RSC Adv.*, 2020,**10**, 38281.
12. C. Rizzo, P. Cancemi, L. Mattiello, S. Marullo, F. Anna, *ACS Appl. Mater. Interfaces*, 2020, **12**, 48442.
13. M. Havlík, V. Talianová, R. Kaplánek, T. Bříza, B. Dolenský, J. Králová, P. Martásek, V. Král, *Chem. Commun.*, 2019, **55**, 2696.
14. A.H. Day, J. Domarkas, S. Nigam, I. Renard, Ch. Cawthorne, B.P. Burke, G.S. Bahra, P.C. F. Oyston, I.A. Fallis, S.J. Archibald, S.J.A. Pope, *Dalton Trans*., 2020, **49**, 511.
15. J. Shi, Y. Wang, X. Tang, W. Liu, H. Jiang, W. Dou, W. Liu, *Dyes and Pig*., 2014, **100**, 255.
16. L.M. Groves, C.F. Williams, A.J. Hayes, B.D. Ward, M.D. Isaacs, N.O. Symonds, D. Lloyd, P.N. Horton, S.J. Coles, S.J. A. Pope, *Dalton Trans.*, 2019, **48**, 1599.
17. M.D.Tomczyk, K.Z.Walczak, *European Journal of Medicinal Chemistry*, 2018,**159**, 393.
18. M. Poddar, V. Sharma, S.M. Mobin, R. Misra, *Chem. Asian J.*, 2018, **13**, 2881.
19. S. Banerjee, J.A. Kitchen, S.A. Bright, J.E. O'Brien, D.C. Williams, J.M. Kelly, T. Gunnlaugsson, *Chem. Commun.*, 2013, **49**, 8522.
20. S. Banerjee, J.A. Kitchen,T. Gunnlaugsson, J.M. Kelly, *Org. Biomol. Chem.*, 2013, **11**, 5642

21. L.Y. Zhao, Q.L. Mi, G.K. Wang, J.H. Chen, J.F. Zhang, Q.H. Zhao, Y. Zhou, *Tetrahedron Lett.*, 2013, **54**, 26, 3353.

22. D.Y. Liu, J. Qi, X.Y. Liu, H.R. He, J.T. Chen, G.M. Yang, *Inorg Chem Commun*., 2014, **43**, 173.

23. Z. Li, W. Chen, L. Dong, Y. Song, R. Li, Q. Li, D. Qu, H. Zhang, Q. Yang, Y. Li, *New J. Chem.*, 2020, **44**, 3261.

24. W. Wang,Q. Wen, Y. Zhang, X. Fei, Y. Li, Q. Yang, X. Xu, *Dalton Trans.*, 2013,**42**, 1827.

25. P. Gopikrishna, N. Meher, P.K. Iyer, *ACS Appl. Mater. Interfaces*, 2018,**10**, 12081.

26. H. Wang, E. Zhao, J.W.Y. Lam, B.Z. Tang, *Materials Today*, 2015,**18**, 365.

27. J. Dai, Ch. Duan, Y. Huang, X. Lou, F. Xia, S. Wang, *J. Mater. Chem. B.*, 2020,**8**, 3357.

28. G. Chen, Z. Zhou, H. Feng, Ch. Zhang, Y. Wang, Z. Qian, J. Pan,*Chemical Communications*, 2019,**55**, 4841.

29. X. Cai, B. Liu, *Angew.Chem. Int. Ed.*, 2020, **59**, 9868.

30. R. Maragani, R. Sharma, R. Misra, *ChemistrySelect*, 2017, **2**, 10033.

31. R. Misra, T. Jadhav, B. Dhokale, S.M. Mobin, *Chem. Commun.*, 2014, **50**, 9076.

32. H.H. Lin Y.Ch. Chan, J.W. Chena, Ch.Ch. Chang,*J. Mater. Chem.*, 2011,**21**, 3170.

33. N. Meher S. Panda, S. Kumar, P.K. Iyer,*Chem. Sci*.,2018,**9**, 3978.

34. M. Li F. Du, P. Xue, X. Tan, S. Liu, Y. Zhou, J. Chen, L. Bai, *Spectrochimica Acta Part A: Molecular and Biomolecular Spectroscopy*, 2020,**227**, 117760.

35. M. Soni, S.K. Das, P.K. Sahu, U.P. Kar, A. Rahaman, M. Sarkar, *J. Phys. Chem. C.*, 2013, **117**, 14338.

36. Y. Li Y. Wu, J. Chang, M. Chen, R. Liu, F. Li, *Chem. Commun.*, 2013, **49**, 11335.

37. S. Mukherjee, P. Thilagar, *Chem. Eur. J*., 2014, **20**, 9052.

38. B.K. Dwivedi, R.S. Singh, A.Ali, V. Sharma, S.M. Mobin, D.S. Pandey, *Analyst*, 2019,**144**, 331.

39. V.S. Padalkar, S. Seki, *Chem. Soc. Rev.*, 2016,**45**, 169.

40. J. Zhao, H. Dong, H. Yang, Y. Zheng. Aggregation Promotes Excited-State Intramolecular Proton Transfer for Benzothiazole-Substituted Tetraphenylethylene Compound. *ACS Appl. Bio Mater.* 2, 2019, 5182.

41. D. Kolosov, V. Adamovich, P. Djurovich, M.E. Thompson, Ch. Adachi, *J. Am. Chem. Soc.*, 2002, **124**, 9945.

42. W. Zhang, Y. Xu, M. Hanif, S. Zhang, J. Zhou, D. Hu, Z. Xie, Y. Ma,*J. Phys. Chem. C*, 2017,**121**, 23218.

43. M. Poddar, G. Sivakumar, R. Misra, *J. Mater. Chem. C*, 2019, **7**, 14798.

44. R.K. Meka M.D. Heagy, *J. Org. Chem.*, 2017, **82**, 12153.

45. P.A.Panchenko Y.V. Fedorov, O.A. Fedorova, *Journal of Photochemistry and Photobiology A: Chemistry*, 2018, **364**, 124.

46. J. Gan, K. Chen, Ch.P. Chang, H. Tian, *Dyes and Pigments*, 2003,**57**, 21.

47. J. Ma, J. Zhao, P. Yang, D. Huang, C. Zhanga, Q. Lia, *Chem. Commun.*, 2012,**48**, 9720.

48. Y. Fang, Y. Zhou, J.Y. Li, Q.Q. Rui, Ch. Yao, *Sensors and Actuators B: Chemical*, 2015,**215**, 350.

49. X. Song M. Wang, L. Kongc, J. Zhao, *RSC Adv.*, 2017,**7**, 18189.

50. Ch.W. Lee, J.A. Seo, M.S. Gong, J.Y. Lee,*Chem. Eur. J.*, 2013, **19**, 1194.

51. L. Wang M. Fujii, M. Yamaji, H. Okamoto,*Photochem. Photobiol. Sci.*,2018,**17**, 1319.

52. M. Korzec S. Kotowicz, R. Rzycka-Korzec, E. Schab-Balcerzak, J.G. Małecki, M. Czichy, M. Łapkowski,*J Mater Sci.*, 2020, 55, 3812.

53. P. Kucheryavy, G. Li, S. Vyas, Ch. Hadad, K.D. Glusac, *J. Phys. Chem. A.*, 2009,**113**, 6453.

54. D. Gudeika, *Synthetic Metals.*, 2020, **262**, 116328.

55. M. Korzec, S. Senkała, R. Rzycka-Korzec, S. Kotowicz, E. Schab-Balcerzak, J. Polański, *Journal of Photochemistry & Photobiology A: Chemistry*, 2019,**382**, 111893.

56. S. Senkała, J.G. Małecki, M. Vasylieva, A. Łabuz, K. Nosek, K. Piwowarczyk, J. Czyż, E. Schab-Balcerzak, H. Janeczek, M. Korzec, *Journal of Photochemistry and Photobiology B: Biology*, 2020,**212**, 112020.

57. M.P. Romero-Fernández M. Ávalos, R. Babiano, P. Cintas, J.L. Jiménez, M.E. Lightb, J.C. Palaciosa, *Org. Biomol. Chem.*, 2014,**12**, 8997.

58. E. Schab-Balcerzak, M. Siwy, M. Filapek, S. Kula, G. Malecki, K. Laba, M. Lapkowskia, H. Janeczek, M. Domanski, *Journal of Luminescence*, 2015,**166**, 22.

59. R. Hu, S. Li, Y. Zeng, J. Chen, S. Wang, Y. Li, G. Yang,*Phys. Chem. Chem. Phys.*, 2011, **13**, 2044.

60. B.K. Dwivedi, V.D. Singh, R.P. Paitandi, D.S. Pandey, *J. Phys. Chem. C.*, 2020,**124**, 15523.

61. P. Bujak I. Kulszewicz-Bajer, M. Zagorska, V. Maurel, I. Wielgusa, A. Pron, *Chemical Society Reviews*, 2013, **42**, 8895.

62. Ł. Skórka, P. Kurzep, G. Wiosna-Sałyga, B. Łuszczyńska, I. Wielgus, Z. Wróbel, J. Ulański, I. Kulszewicz-Bajera, *Synthetic Metals*, 2017,**228**, 1.

63. I. Glowacki, Z. Szamel., *J. Phys. D: Appl. Phys.*, 2010,**43**, 295101.

64. K. Kotwica P. Bujak, D. Wamil, A. Pieczonka, G. Wiosna-Salyga, P.A. Gunka, T. Jaroch, R. Nowakowski, B. Luszczynska, E. Witkowska, I. Glowacki, J. Ulanski, M. Zagorska, A. Pron, *J. Phys. Chem. C.*, 2015,**119**, 10700.

65. S.A.Hussain, 2009, arXiv:0908.1815.

66. A. Ettinger, T. Wittmann, *Methods in cell biology*, 2014, **123**,77

67. Z. Wang, S. Chen, J.W.Y. Lam, W. Qin, R.T.K. Kwok, N. Xie, Q. Hu, B.Z. Tang, *J. Am. Chem. Soc*., 2013, **135**, 8238.

Highligts:

- Properties of 1,8-Naphthalimide derivatives with imine and β-ketoenamine bonds were compared,
- Thermal, electrochemical and optical investigation were preformed,
- The β-ketoenamine derivatives exhibited aggregation-induced emission (AIE),
- The analyzed derivatives were used in OLEDs and in cell imaging,